

Fatigue strength improvement method for thin sheet GMA welding joints by weaving

Matsuda, Kazuki
Kyushu University

Ishida, Yoshinari
Nippon Steel Corporation

Kodama, Shinji
Nippon Steel Corporation

<https://hdl.handle.net/2324/6758694>

出版情報 : Welding in the World, 2023-01-23. Springer
バージョン :
権利関係 :

Title: Fatigue strength improvement method for thin sheet GMA welding joints by weaving

Kazuki Matsuda*

Kyushu University, Motoooka 744, Nishi-ku, Fukuoka, 819-0395, Japan (Formerly Nippon Steel Corporation)

E-mail: matsuda@nams.kyushu-u.ac.jp

ORCID: 0000-0003-3227-8413

*Corresponding author

Yoshinari Ishida, Shinji Kodama

Nippon Steel Corporation, 20-1 Shintomi, Futtsu, Chiba prefecture, 293-8511, Japan

Abstract:

A method for improving the fatigue strength of thin steel sheet gas metal arc (GMA) welded joints using weaving welding was evaluated. Weaving created peaks and valleys at the weld toe. The valley has high stress triaxiality, and plastic deformation is unlikely to occur. Fatigue cracks occurred from the peaks with gentle toe shapes. Therefore, it is considered that the fatigue strength is improved by reducing the initiation points of the crack and stress concentration at the toe. The fatigue test results showed that the fatigue limit of the weaving welding joint was improved compared with that of the normal welding joint. Furthermore, the optimal weaving condition, which is the relationship between the weaving wavelength and torch swing amplitude, was evaluated. As a consequence, when the wave density is small, the crack initiation point is not restricted to the peak. On the other hand, when the wave density is large, the peak and valley shapes merge and the weaving effect disappears. In addition, undercuts occurred when the swing amplitude became too large. The mechanism of improving the fatigue strength was considered by observing the initiation point of the fatigue microcracks.

Keywords:

Weaving, microcracks, lap fillet welding joint, GMA welding, fatigue, hot-rolled steel sheet

Statements and Declarations:

There are no conflicts of interest to declare.

Author contributions:

All authors contributed to the study conception and design. Material preparation, data collection and analysis were performed by Kazuki Matsuda. The first draft of the manuscript was written by Kazuki Matsuda and all authors commented on previous versions of the manuscript. All authors read and approved the final manuscript.

1. Background

Gas metal arc (GMA) welding is the primary method for joining automobile chassis members. Fatigue strength is significant for GMA-welded parts of chassis members. Ultrasonic impact treatment (UIT) [1] and shot blast treatment [2] are effective in improving fatigue strength. However, it is difficult to apply because of the increase in processes and the cost of introducing equipment.

Otegui et al. [3] reported that weld beads produced by automated welding have inferior high-cycle fatigue strength compared to beads produced by manual welding. Verreman et al. [4] reported that, in a weld bead produced by manual welding, an irregular ripple occurs near the toe, which is the fatigue crack initiation point, and the crack propagates in a complex coalescing manner. Chapetti et al. [5] attempted to reproduce the ripple of manual welding using arc rotation. In the periodically fluctuating toe shapes shown in Figure 1, the valley region has high stress triaxiality and is less likely to be subject to plastic deformation. Cracks were generated in the peak region, and it was found that the cracks required a number of cycles to coalesce owing to interference between the generated and propagating cracks. Thus, it has been reported that the main factor for fatigue life extension is the retardation of crack propagation. Skriko et al. [6] reported that fatigue strength was increased by fatigue tests on weaving-welded cruciform joint specimens. They believed that the extension of propagation life had a significant influence on the fatigue life extension, but the initiation life was over 80% of the total life. They also considered that the main factor of the fatigue life extension was the gentle toe shape caused by weaving welding. Duchet et al. [7] reported that the fatigue strength

of automotive steel sheets was improved by weaving welding. They considered that the reason for the improvement in fatigue strength was the increase in bead width and the improvement in the toe shape.

Generally, the thinner the sheet, the greater the ratio of the crack initiation life to the total fatigue life. Ottersböck et al. [8] performed fatigue tests on butt-welded joints with a sheet thickness of 6 mm and reported that 50% of the fatigue life was spent before the crack reached a depth of 0.5 mm. Thus, it can be inferred that delaying crack coalescence of the welds by cyclic ripple is not effective in extending the fatigue life of thin sheet arc welds. As mentioned above, the gentle toe shape is often believed to be the primary factor in extending the crack initiation life. However, the surface irregularity of the weld metal in the vicinity of the toe in the arc welds of thin steel sheets reduces the fatigue strength [9-11]. Thus, even if the macroscopic toe shape is smoothed, fatigue strength may not be effectively improved in high-strength welds. However, If the fatigue crack initiation point can be limited to the peak region shown in Figure 1, the fatigue strength can be sufficiently improved even in ultra-high-tensile-strength thin-sheet arc welds. Assuming arc welding by an articulated robot for automobile chassis members, weaving is considered a suitable means of intentionally creating such waviness at the weld toe. In this study, a fatigue strength improvement method using weaving was evaluated for thin-sheet lap-fillet arc welds.

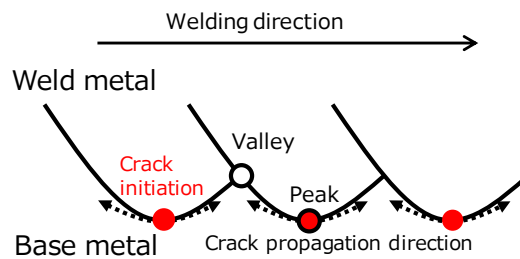


Figure 1 Schematic diagram of weaving weld bead.

2. Experiment

A lab-hot-rolled steel sheet with a sheet thickness is 2.9 mm is used in this study. The mechanical properties of the material is shown in Table 1. The welding wire used was a general-purpose solid wire for 490 MPa grade steel and the diameter of the wire was 1.2 mm. The mechanical properties of deposited metal is shown in Table 2

A schematic of the welding process is shown in Figure 2 and the arc welding and weaving setup conditions are listed in Table 3, respectively. The joint type was a lap-fillet joint as shown in Figure 2. To determine the effects of the torch swing range and toe wave density on the fatigue strength, the welding conditions were varied, as shown in Table 3. Although welding

was also performed at a range of 4.5 mm, undercut occurred at the toe, and this was excluded from the fatigue evaluation described below.

Table 1 Mechanical properties of the steel sheet.

0.2% proof stress	Tensile strength	Elongation
[MPa]	[MPa]	[%]
729	803	17.4

Table 2 Mechanical properties of the deposited metal. (Shield gas: Ar + 20%CO₂)

0.2% proof stress	Tensile strength	Elongation
[MPa]	[MPa]	[%]
460	570	30

Table 3 Welding conditions.

Current	Voltage	Welding speed	Weaving parameter		
			Frequency	Range	Wave density
A	V	m/min	Hz	mm	Wave /20 mm
235	27.2	0.8	2.0	2.5	3.0
176	24.5	0.6	2.0	2.5	4.0
176	24.5	0.6	2.5	2.5	5.0
176	24.5	0.6	3.0	2.5	6.0
176	24.5	0.6	2.5	3.5	5.0
176	24.5	0.6	3.0	3.5	6.0
176	24.5	0.6	2.5	4.5	5.0
176	24.5	0.6	3.0	4.5	6.0
176	24.5	0.6	0	0	0

A cross-sectional samples were taken from the obtained welded part and observed using optical microscopy. Cross-sectional samples of the weaving welds were taken from two locations, peak and valley. The samples were etched with an aqueous picric acid solution.

The geometry of the specimen used for the fatigue test is shown in Figure 3. The specimens were taken from the welded steel sheets so that the peak portion of the wave at the weld toe was located at the edge of the specimen. The fatigue test was a Schenck type displacement-controlled plane bending load (stress ratio $R = 0.1$, convex upward in Figure 3). The specimen was fixed at one end and the out-of-plane displacement (z -direction) was loaded at the other end. The load cell is located at the fixed end. The bending moment was calculated by multiplying the reaction force by the length of the specimen. The loading frequency is 25 Hz. Failure was defined as a decrease in the bending moment to less than 50 % of the initial moment. The stress range, $\Delta\sigma$, is the difference between the maximum and minimum stresses. The maximum and minimum stresses are based on the bending stress of the surface σ , which was calculated using the width B of the center of the specimen, sheet thickness t , and bending moment M . From these values, $\sigma = 6M/(Bt^2)$. The fatigue limit was defined as a non-fracture stress range of 10^7 cycles. It is generally said that the fatigue strength of a welded part is affected by the residual stress. However, it is known that the effect of residual stress is small [10, 11] in a thin-sheet arc welded part. Therefore, residual stress was not considered in this study.

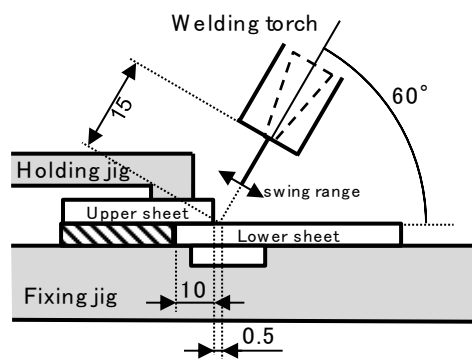


Figure 2 Schematic illustration of lap fillet welding

Microcracks in specimens that did not fail after 10^7 cycles loading were examined to determine the fatigue crack initiation point in thinsheet arc welded part. The observed sites were the midpoint between the valley and peak and the peak position. The specimens observed were in 3, 4, 5, and 6 wave/20 mm conditions with a swing range of 2.5 mm. The purpose of this observation is to examine the location of fatigue cracks by observing cracks with short dimensions that have just initiated. The surface of the arc welds is covered with welding slag, making it impossible to observe the location of fatigue crack initiation

during the fatigue test. Note that no microcracks were observed on the surface of the weld before the fatigue test from the observations in another cross-section samples.

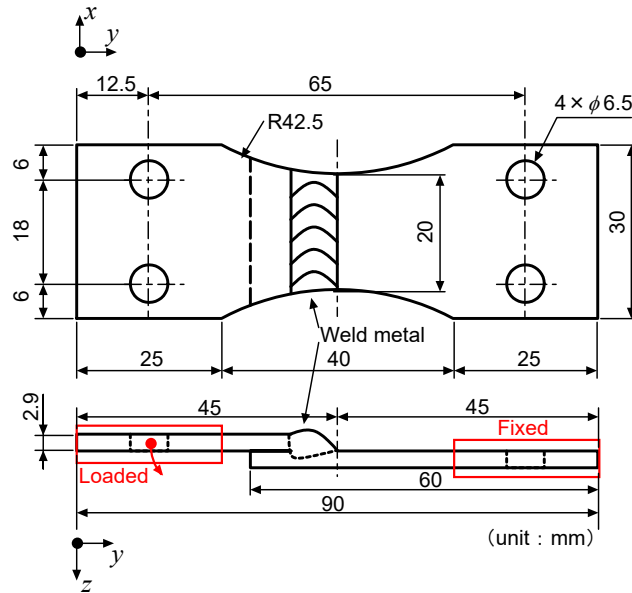
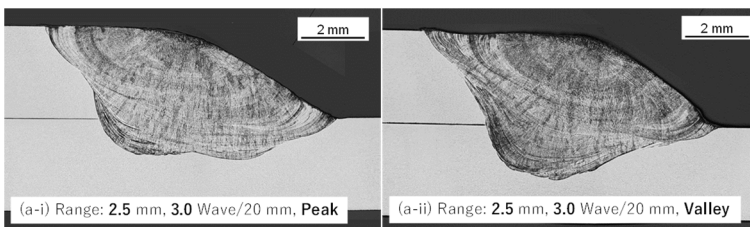


Figure 3 Geometry of the specimen for the fatigue test.

3. Results

3.1 Observation of welded cross-sections

The entire welded cross-sectional shape is shown in Figure 4. (a) - (h) Weaving welds show a gentler toe shape than (i) normal (no weaving) welds. In many cases, the peak cross-section is gentler than the valley cross-section. In addition, the larger the swing range, the larger the bead width and the shallower the penetration. The results for a swing range of 4.5 mm showed that undercut occurred in the valley regardless of the wave density.



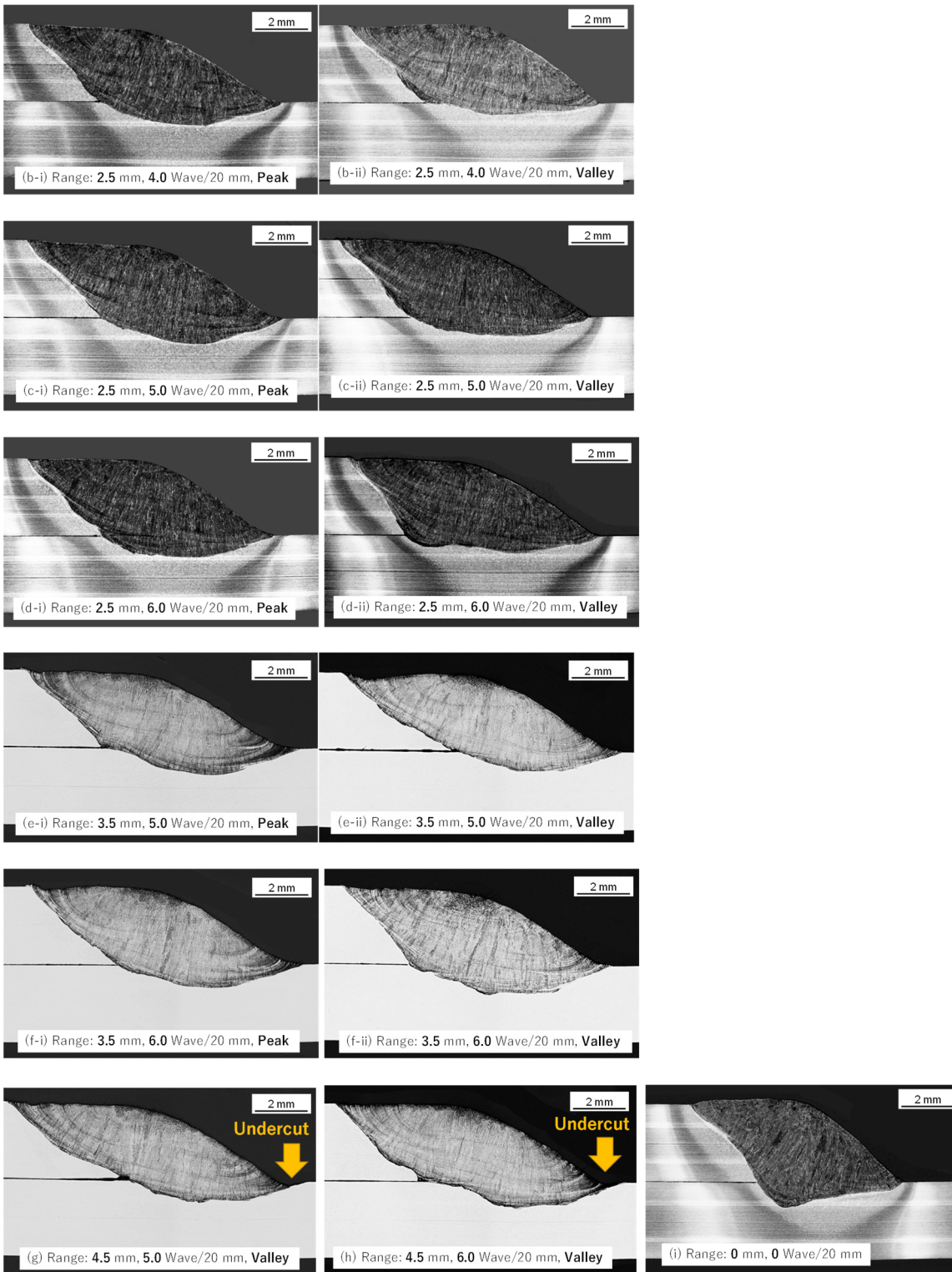


Figure 4 Optical microscope images of welded cross-sections.

3.2 Fatigue test and observation of microcracks

The S-N diagram obtained from the fatigue tests is shown in Figure 5. The fatigue strength and standard deviation for each test condition is listed in Table 4. The standard deviation was calculated using the ruptured plot of the S-N diagram in Figure 4. The fatigue strength improved in many cases with weaving compared to that without weaving. Figure 6 shows an example of the observation results for microcracks in a specimen that did not fail in the fatigue test. Fatigue cracks were observed on the surface of the weld metal in the vicinity of the toe. Table 5 lists the cross-sections where microcracks were observed. At 3 waves/20 mm, microcracks were observed at the midpoint between the peaks and valleys. No microcracks were observed at 4 waves/20 mm. Microcracks were observed in the peaks at 5 and 6 waves/20 mm, respectively. From these results, it can be presumed that the higher the wave density, the closer the location of fatigue crack initiation is to the peak.

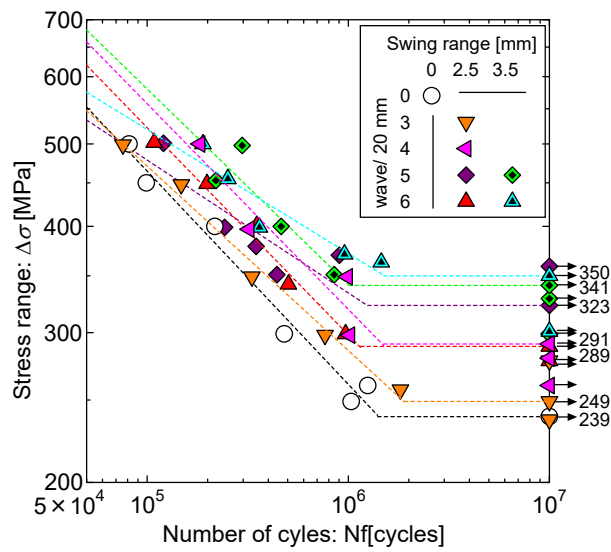


Figure 5 S-N curves

Table 4 List of fatigue strengths (standard deviation) for each condition.

		Swing range [mm]		
		0	2.5	3.5
Wave density [Wave/ 20mm]	0	239 (± 13.9)	-	-
	3	-	249 (± 10.0)	-
	4	-	291 (± 23.2)	-

	5	-	323 (± 26.8)	341 (± 28.3)
	6	-	289 (± 10.3)	350 (± 19.1)

Table 5 Microcrack observation results (swing range 2.5mm)

Wave /20 mm	Cross-section	
	Midpoint	Peak
3	○	-
4	-	-
5	-	○
6	-	○

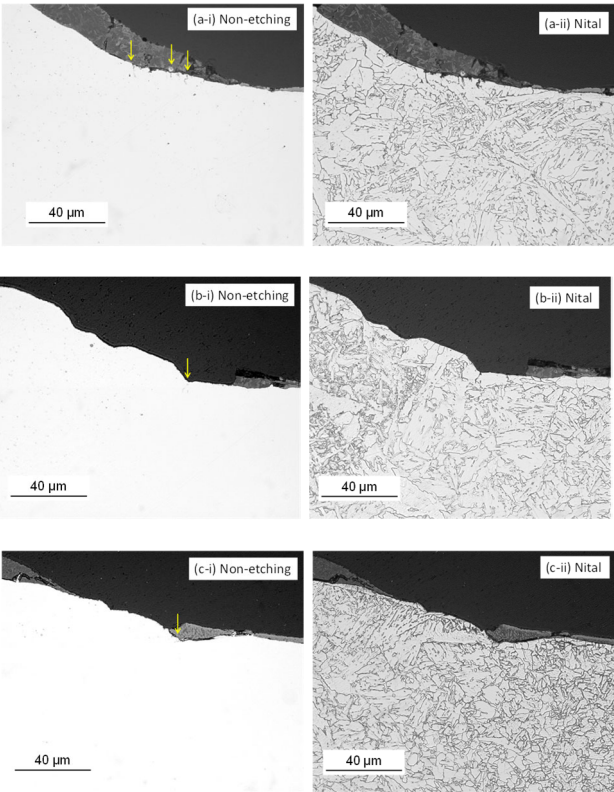


Figure 6 An example of microcrack observations. (a) Midpoint (3 wave/20 mm), (b) Peak (5 wave/20 mm), (c) Peak (6 wave/20 mm).

4. Discussion

The relationships between the swing range, number of waves per 20 mm, and fatigue limit are shown in Figure 7. It can be observed that the improvement in the fatigue limit due to weaving increases with increasing wave density and decreases after reaching a maximum value. The fatigue strength of the weaving welds was not always associated with the toe shapes at peak cross-section of the weaving welds, even though the toe shapes at peak cross-section of the weaving welds were all gentler than those of the welds without weaving. This is thought to be due to the fact that the position of fatigue crack initiation varies depending on the welding conditions, as shown in the microcrack observation photographs in Figure 6. The wave density at which the maximum improvement in the fatigue limit was obtained changed as the swing range increased. A schematic of the effect of the weaving wave density on the fatigue strength, as considered from the change in fatigue limit and the observation of microcracks, is shown in Figure 8. If the wave density is appropriate (5 waves/20 mm), then the fatigue limit improvement effect can be obtained. This is because the deformation constraint at the valley acts and the cracks only originate from the peak cross-section which have gently toe shapes. However, when the wave density was small (3 waves/20 mm), the deformation restraint at the valley was small, and the crack initiated midway between the peak and valley. At this position, the toe shape is between the steep valley and gentle peak, and the effect of reducing the stress concentration is considered to be small. Therefore, the effect of fatigue strength improvement was small. However, when the wave density is dense (6 waves/20 mm), the shapes of the peaks and valleys merge, and the weaving effect itself is considered to be small.

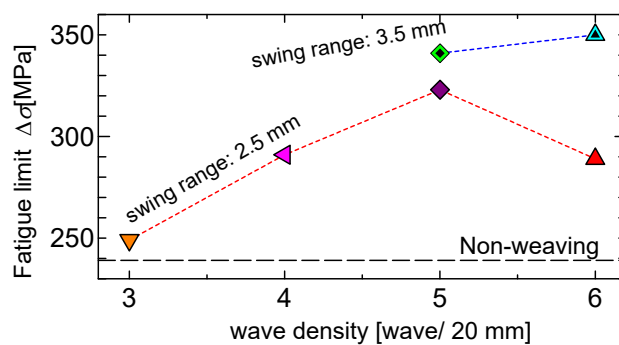


Figure 7 Relationship between wave density and fatigue limit

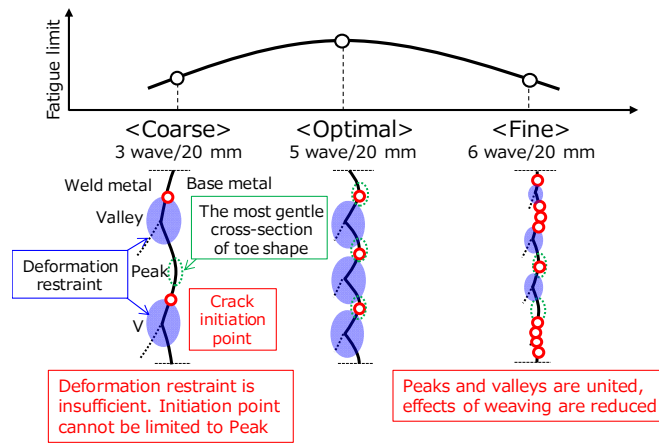


Fig.8 Schematic diagram of the relationship between wave density and fatigue limit

A schematic of the relationship with the fatigue limit, with the swing range added to the relationship in Figure 8, is shown in Figure 9. Increasing the swing range is expected to influence the occurrence of the weaving effect even at high wave densities. However, an excessive increase in the swing range is expected to increase the likelihood of defects such as undercuts at the weld toe. The weaving welding under the appropriate range of conditions described above is considered to effectively improve fatigue strength. This research studied the effect of weaving weld geometry on fatigue strength. In addition, the effect of weaving conditions on the weaving geometry was also investigated. Generally, fatigue strength is also affected by microstructure and material strength. Therefore, it is necessary to consider these factors in order to quantitatively estimate the fatigue strength. Based on the knowledge obtained in this study, it is important to determine the cross-sectional location of fatigue cracks initiation in weaving welds. It is recommended that a fatigue strength evaluation method [12, 13] should be applied to that cross-section.

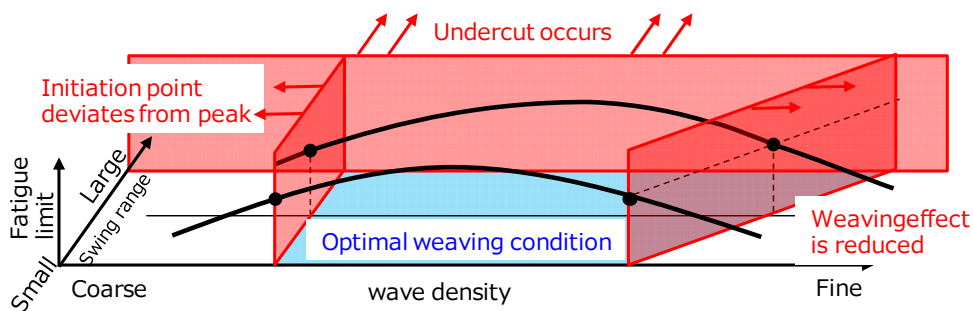


Figure 9 Relationship between wave density, swing range, and fatigue limit

5. Conclusion

In this study, a fatigue strength improvement method using weaving was evaluated for thin-sheet lap-fillet welds. The conclusions are as follows:

- Both the fatigue life and fatigue limit were improved by weaving welding compared to conventional welding.
- Crack initiation at the valley of the toe was suppressed by the deformation restraint, and crack initiation from the gentle peak was considered to improve the fatigue strength.
- The appropriate range of conditions and mechanisms for improving the fatigue strength with respect to the wave density and swing range of weaving are discussed.

References

- [1] T. Nose: Ultrasonic Peening Method for Fatigue Strength Improvement, *J. Jpn. Weld. Soc.*, 77, 3, pp.210-213, 2008.
<https://doi.org/10.2207/jjws.77.210>
- [2] H. Fujimoto, K. Akioka and M. Tokunaga: Effects of Shot Blasting on Corrosion Properties after Electrodeposition and Fatigue Properties of Arc Welds in Automotive Steel Sheets, *Mater. Trans.* 58, 12, pp.1715-1720, 2017.
<https://doi.org/10.2320/matertrans.P-M2017838>
- [3] J.L. Otegui, H.W. Kerr, D.J. Burns and U.H. Mohaupt: Fatigue Crack Initiation from Defects at Weld Toes in Steel, *Int. J. Pres. Ves. Pip.*, 38, 5, pp.385-417, 1989. [https://doi.org/10.1016/0308-0161\(89\)90048-3](https://doi.org/10.1016/0308-0161(89)90048-3)
- [4] Y. Verreman and B. Nie: Short Crack Growth and Coalescence along the Toe of a Manual Fillet Weld, *Fatigue Fract. Eng. M.*, 14 2-3, pp.337-349, 1991. <https://doi.org/10.1111/j.1460-2695.1991.tb00663.x>
- [5] M.D. Chapetti and J.L. Otegui: Controlled Toe Waviness as a Means to Increase Fatigue Resistance of Automatic Welds in Transverse Loading, *Int. J. Fatigue*, 19, 10, pp.667-675, 1997. [https://doi.org/10.1016/S0142-1123\(97\)00061-3](https://doi.org/10.1016/S0142-1123(97)00061-3)
- [6] Skriko, T., Björk, T. & Nykänen, T.: Effects of weaving technique on the fatigue strength of transverse loaded fillet welds made of ultra-high-strength steel, *Weld World* 58, 377–387, 2014. <https://doi.org/10.1007/s40194-014-0123-1>
- [7] M. Duchet J. Haouas, E.Gibeau, F. Pechenot et al.: Improvement of the fatigue strength of welds for lightweight chassis application made of Advanced High Strength Steels, *Procedia Struct. Integr.* 19, pp.585–594, 2019.
<https://doi.org/10.1016/j.prostr.2019.12.063>

- [8] M. J. Ottersböck, M. Leitner, M. Stoschka, W. Maurer: Crack Initiation and Propagation Fatigue Life of Ultra High-Strength Steel Butt Joints, *Appl. Sci.*, 9, 21, 4590, 2019. <https://doi.org/10.3390/app9214590>
- [9] B. Schork, P. Kucharczyk, M. Madia, U. Zerbst et al.: The effect of the local and global weld geometry as well as material defects on crack initiation and fatigue strength, *Eng. Fract. Mech.*, 198, pp.103-122, 2018. <https://doi.org/10.1016/j.engfracmech.2017.07.001>
- [10] T. Shiozaki, N. Yamaguchi, Y. Tamai, J. Hiramoto et al.: Effect of weld toe geometry on fatigue life of lap fillet welded ultra-high strength steel joints, *Int J Fatigue*, 116, pp.409-420, 2018. <https://doi.org/10.1016/j.ijfatigue.2018.06.050>
- [11] T. Nagai, R. Kasai, R. Suzuki, M. Mochizuki et al.: An estimation of factors influencing residual stress characteristics of fillet welded lap joints, *Weld. Int.* 31, 12, pp.920-928, 2017. <https://doi.org/10.1080/09507116.2016.1223239>
- [12] K. Matsuda and S. Kodama: Observation of Fatigue Microcracks and Estimation of Fatigue Strength of a Thin Sheet Arc Welded Part Considering Micro-ripples, *Int. J. Fatigue*, 145, pp.106087, 2021. <https://doi.org/10.1016/j.ijfatigue.2020.106087>
- [13] A.F. Hobbacher: The new IIW recommendations for fatigue assessment of welded joints and components – A comprehensive code recently updated, *Int. J. Fatigue*, 31, 1, pp.50-58, 2009. <https://doi.org/10.1016/j.ijfatigue.2008.04.002>